- Supporting Information -

Copolymerization of Isoprene with *para*-Alkylstyrene Monomers: Disparate Reactivity Ratios and the Shape of the Gradient

Philipp von Tiedemann [a,b], Jan Blankenburg [a,b], Kamil Maciol [a], Tobias Johann [a,c], Axel H. E. Müller [a,], Holger Frey [a,*]*

[a] Institute of Organic Chemistry, Johannes Gutenberg University Mainz, Duesbergweg 10-14, 55128 Mainz, Germany

[b] Graduate School Materials Science in Mainz, Staudinger Weg 9, 55128 Mainz, Germany

[c] Max Planck Graduate Center with the Johannes Gutenberg University, Staudinger Weg 6, 55128 Mainz, Germany

*E-Mail: hfrey@uni-mainz.de, (H.F.), axel.mueller@uni-mainz.de (A.H.E.M.)

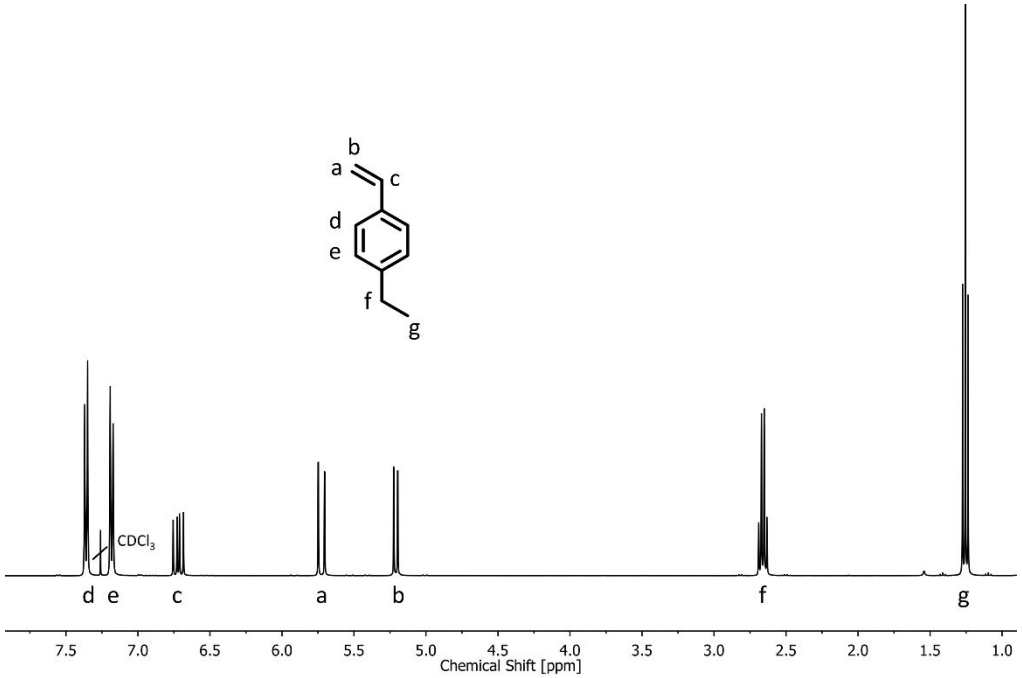

Figure S1. ^{1}H NMR spectrum of *p*-ES (400 MHz, C*D*Cl$_3$).

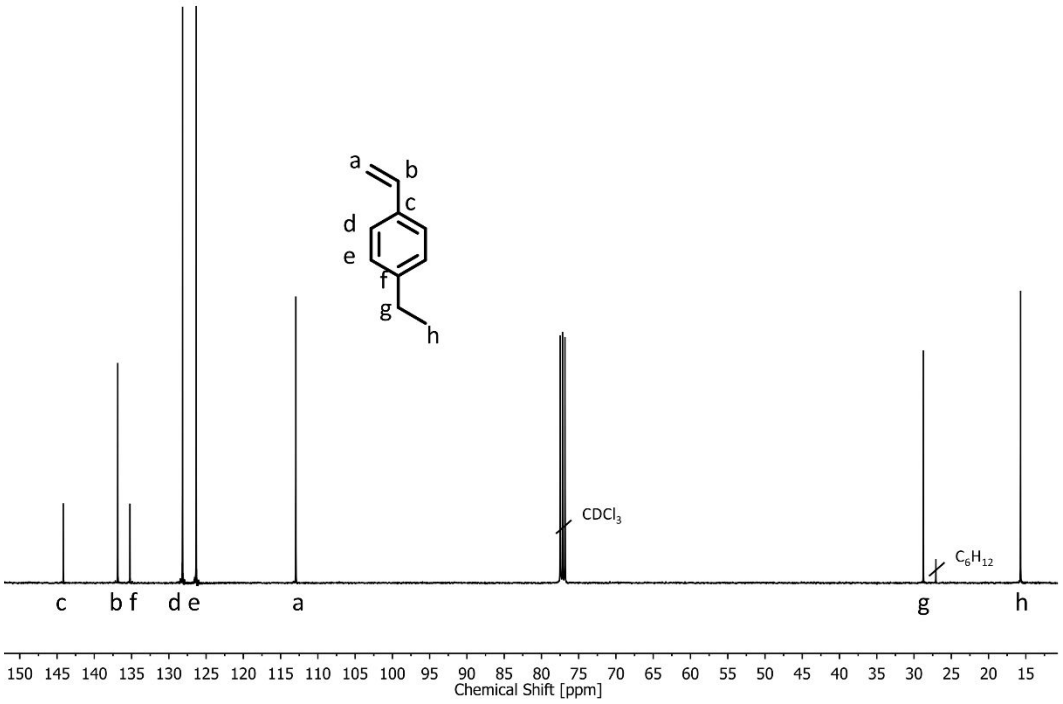

Figure S2. ^{13}C NMR spectrum of *p*-ES (100 MHz, C*D*Cl$_3$).

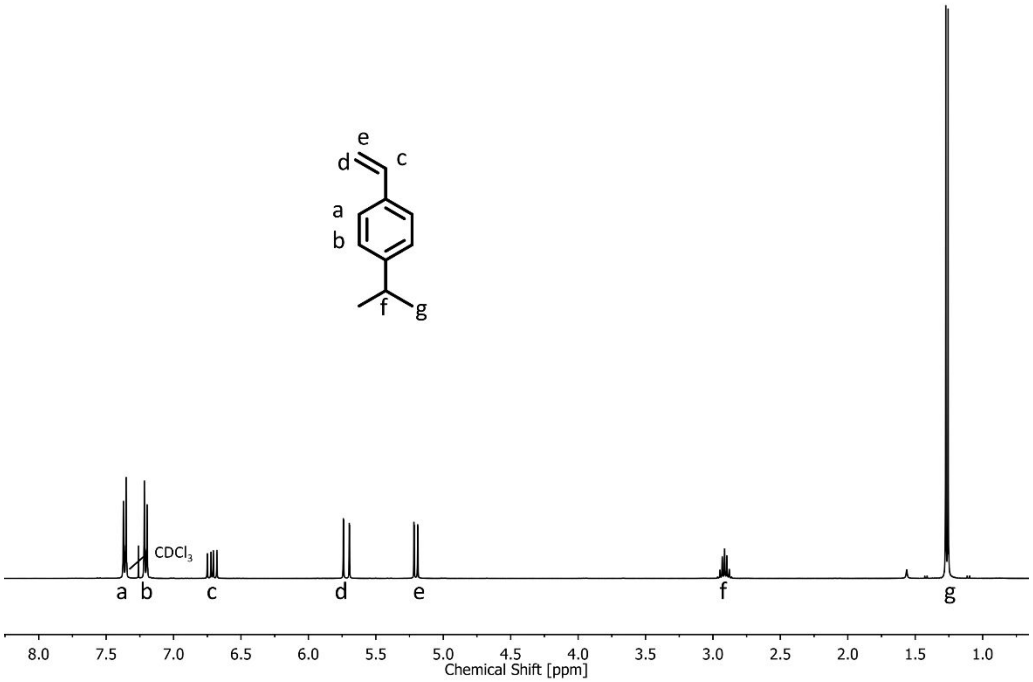

Figure S3. ^{1}H NMR spectrum of *p*-*i*PS (400 MHz, C*D*Cl$_3$).

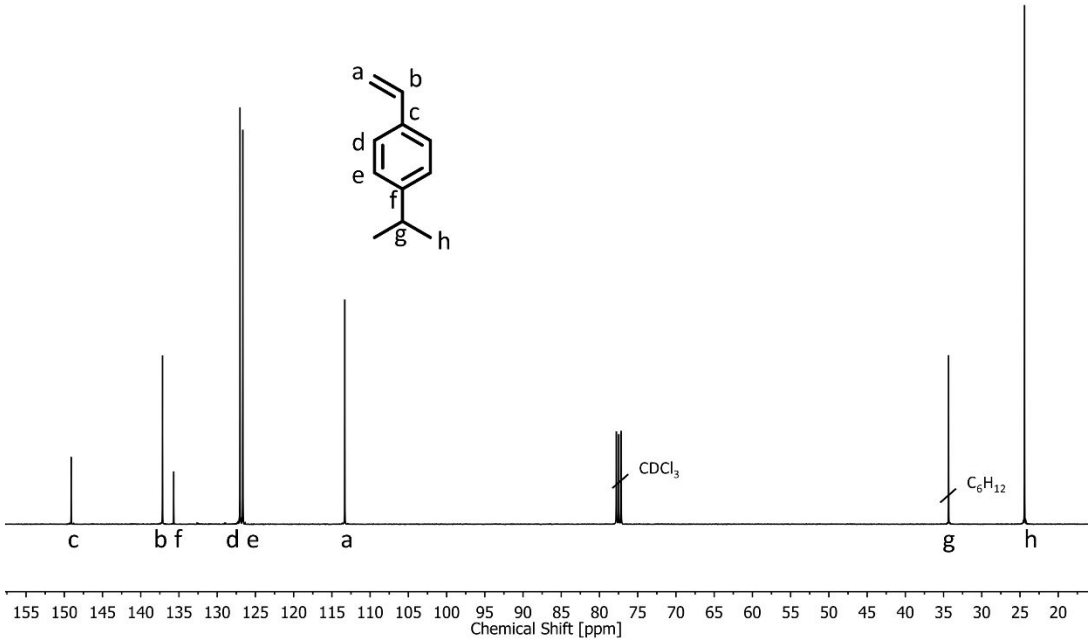

Figure S4. ^{13}C NMR spectrum of *p*-*i*PS (100 MHz, C*D*Cl$_3$).

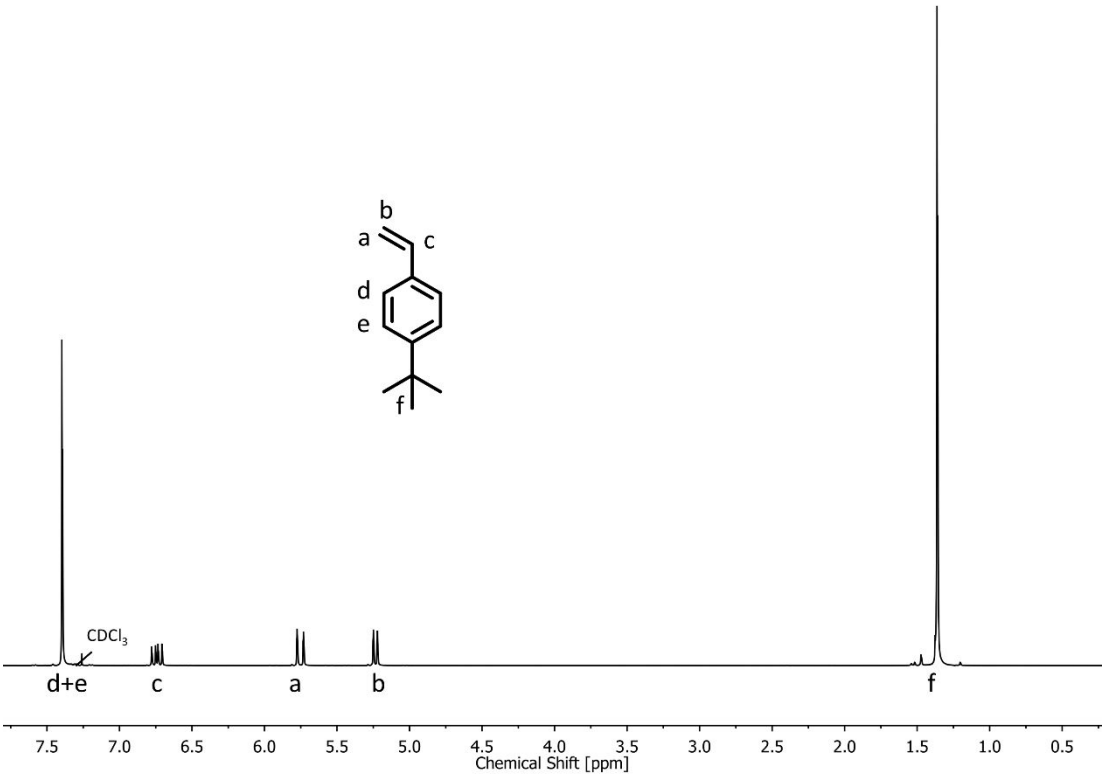

Figure S5. ^{1}H NMR spectrum of *p*-*t*BS (400 MHz, C*D*Cl$_3$).

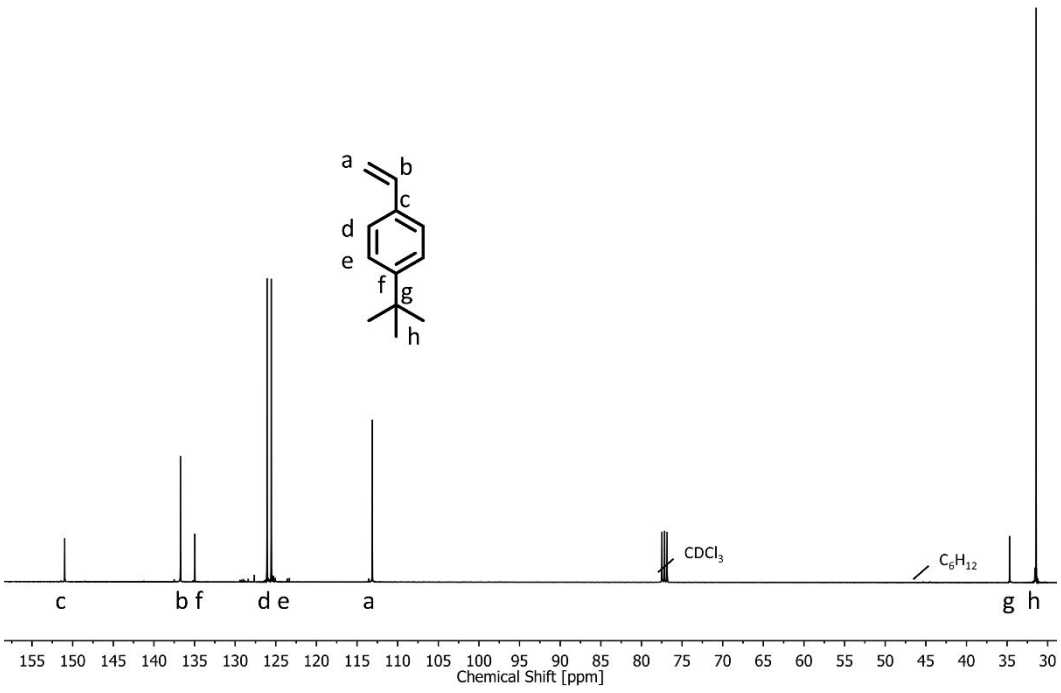

Figure S6. ^{13}C NMR spectrum of *p*-*t*BS (100 MHz, C*D*Cl$_3$).

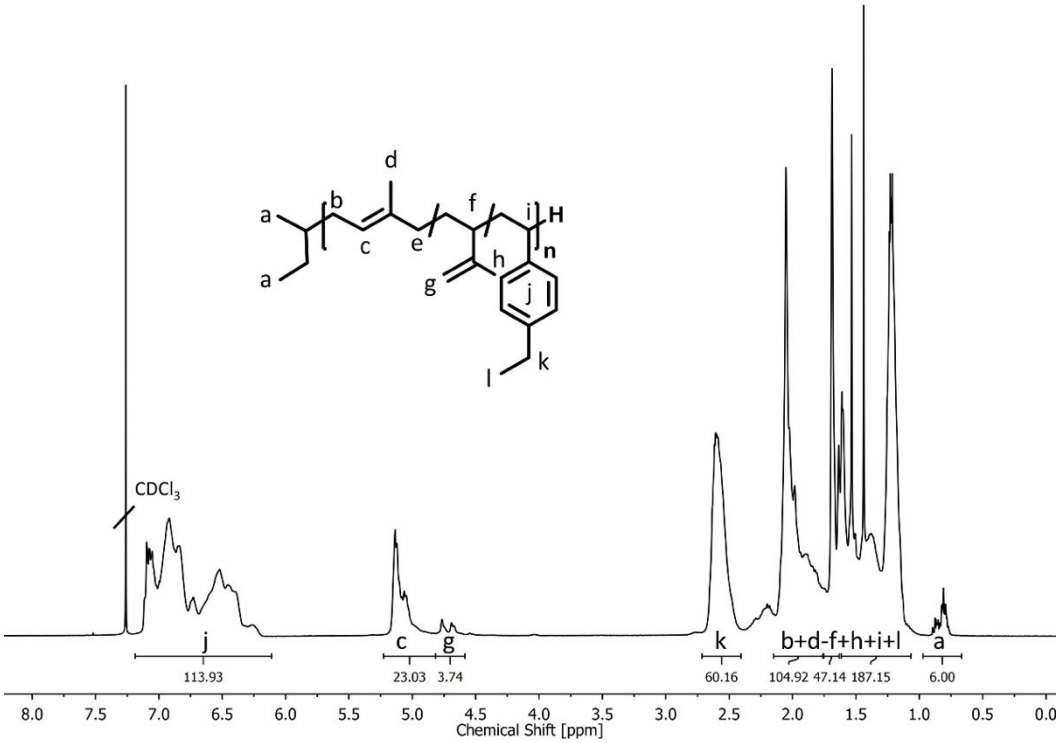

Figure S7. ^{1}H NMR spectrum of P($I_{0.5}$-*grad*-(*p*-ES)$_{0.5}$) (targeted 5,000 g mol^{-1}) (400 MHz, C*D*Cl$_3$).

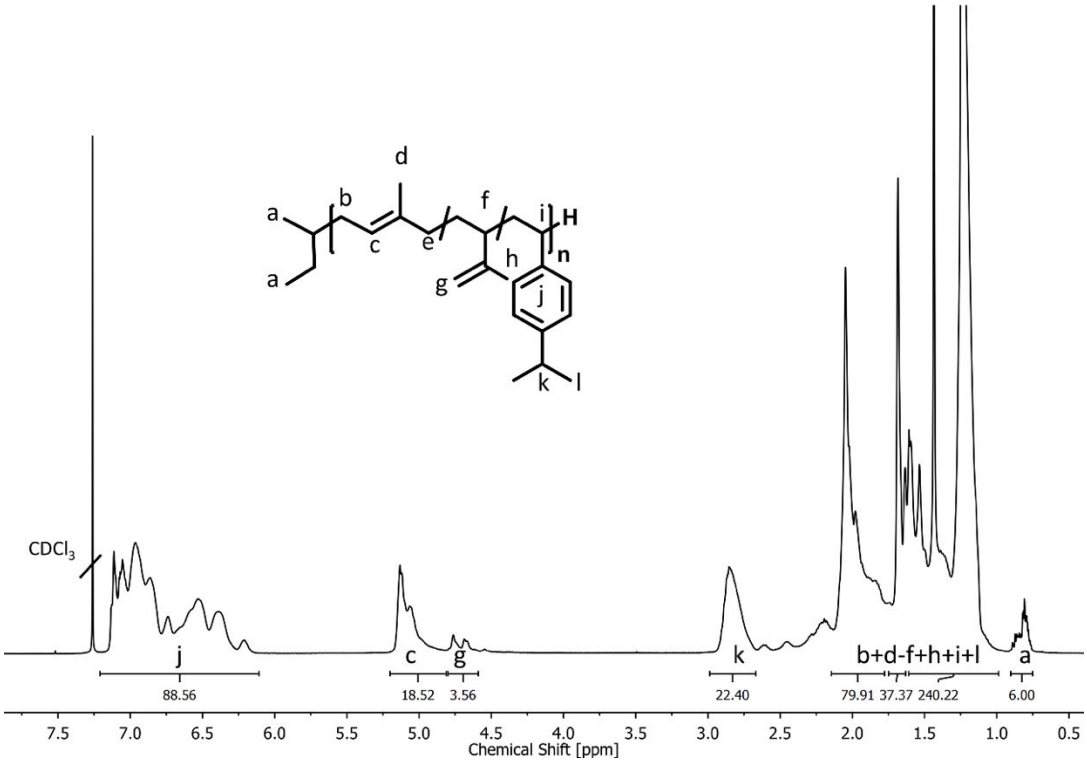

Figure S8. ^{1}H NMR spectrum of P($I_{0.5}$-*grad*-(*p*-*i*PS)$_{0.5}$) (targeted 5,000 g mol^{-1}) (400 MHz, C*D*Cl$_3$).

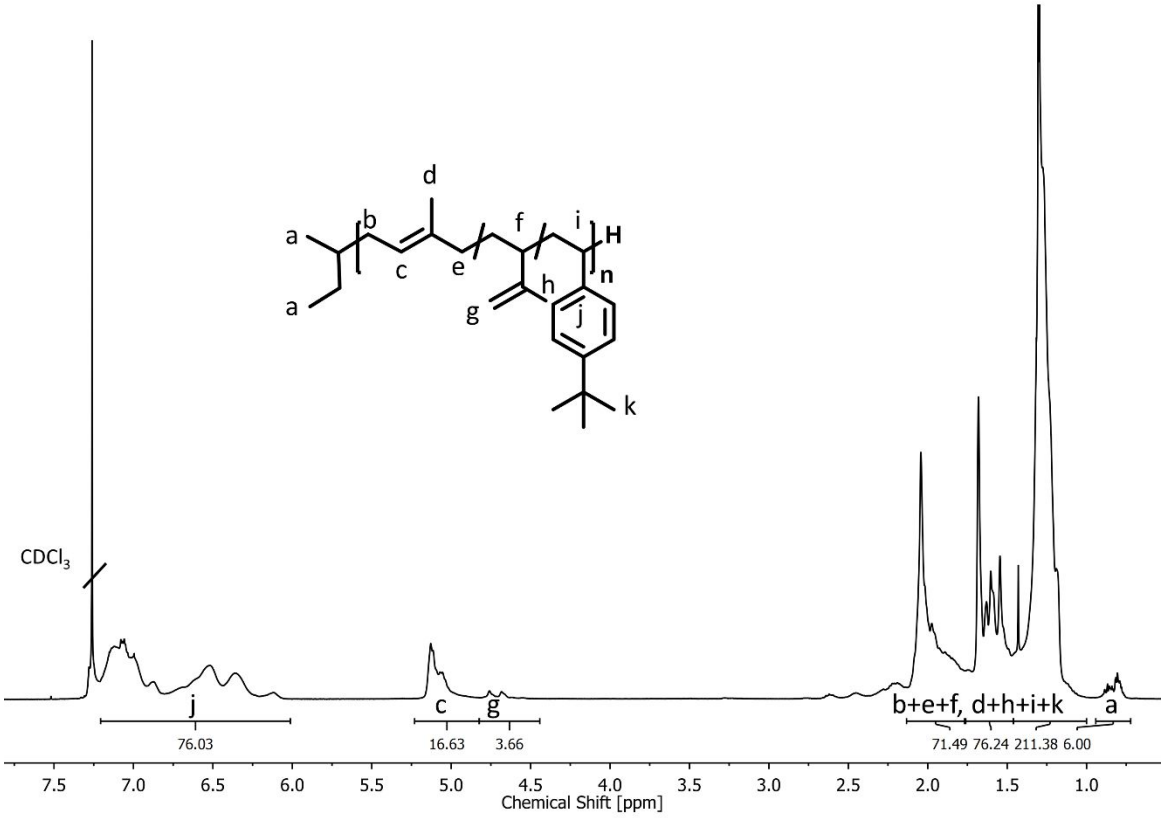

Figure S9. ^{1}H NMR spectrum of P($I_{0.5}$-*grad*-(*p*-*t*BS)$_{0.5}$) (targeted 5,000 g mol^{-1}) (400 MHz, C*D*Cl$_3$).

Determination of the copolymer molecular weight based on SEC measurements with two independent detector signals[1]

For improved accuracy the molecular weights of the copolymers were determined via SEC with two independent detectors signals (UV and RI) with the copolymerization module from the PSS WinGPC® UniChrom (V 8.31, Build 8417) software provided by PSS Polymer Standards Service GmbH.
For the *p*-alkyl styrene comonomers polystyrene standards were employed and for isoprene a series of low dispersity polyisoprene standards was used, for calibration, both provided by PSS.
Using k independent detector signals d, the composition of a copolymer consisting of k comonomers can be determined. For the detector signal U_d as a function of the volume V follows

$$U_d(V) = \sum_d f_{dk} c_k(V)$$

with the response factor f_{dk} of the comonomer k for detector signal d and the concentration of the comonomers c_k in the detector cell at the volume V. In this manner the response

factors were measured for polystyrene and polyisoprene standards at a known concentration injected onto the column.

Table S1. Response factors for polystyrene and polyisoprene.

Detector	Response factor for polystyrene, f_{PS}	Response factor for polyisoprene, f_{PI}
UV (275 nm)	0.1226	0.0005
RI	0.0391	0.0287

In the case of a binary copolymer the weight fraction, W_A, for the comonomer A can be calculated as

$$W_A(V) = \left[1 + \frac{\left[U_1(V) - \frac{f_{1B}}{f_{2B}} \cdot U_2(V)\right]\left[f_{1,A} - \frac{f_{1B}}{f_{2B}} \cdot f_{2A}\right]}{\left[U_1(V) - \frac{f_{1A}}{f_{2A}} \cdot U_2(V)\right]\left[f_{1,B} - \frac{f_{1A}}{f_{2A}} \cdot f_{2B}\right]}\right]^{-1}$$

where in this case for f_{1B}, f_{2B} and f_{1A}, f_{2A} the response factors (UV and RI detectors) for polystyrene and polyisoprene were used as listed above. Thus, by interpolating the calibration curves of the homopolymer standards $M_{PS}(V)$ and $M_{PI}(V)$ and using the weight fractions W_S and W_I for the comonomers styrene (S) and isoprene (I) the molecular weight of the copolymers (M_c) was calculated as

$$\log M_c(V) = W_S(V) log M_S(V) + W_I(V) log M_I(V)$$

and the mean value of the molecular weight (M_n) was calculated for the copolymers as for a conventional GPC by using the above obtained molecular weights.

Evaluation of reactivity ratios via Meyer-Lowry fit

Traditionally, the determination of reactivity ratios was performed by multiple copolymerization experiments with low conversion. The low conversion is essential to assure a constant relative monomer concentration.[2] In copolymerization experiments with similar comonomer reactivity the copolymerization experiment can be subdivided into multiple copolymerization experiments, in which for each interval only a small conversion occurs as shown elsewherere.[3] Applying this technique to the studied copolymerization systems was not sufficantly accurate as shown in Figure S11, S16 and S21 indicated by the reduced R^2 value. The obtained fits produced negative values for r in some cases (r_I = 18.2, $r_{p\text{-}t\text{BS}}$ = -0.008) rendering this method inapplicable. To accurately describe the copolymerization kinetics, the integrated form of the Mayo-Lewis equation needs to be used. The integration of the Mayo-Lewis equation introduced by Skeist and first performed analytically by Meyer-Lowry yields the Meyer-Lowry equation.[2,4] This equation enables the direct fit of the experimental ^{1}H NMR kinetics data to obtain the reactivity ratios. The

following equation was used to fit the compositional drift of f_1 during the total conversion X to determine r_1 and r_2:

$$X = 1 - \left(\frac{f_1}{f_{1,0}}\right)^{\alpha}\left(\frac{1-f_1}{1-f_{1,0}}\right)^{\beta}\left(\frac{f_1-\delta}{f_{1,0}-\delta}\right)^{\gamma}$$

$$\alpha = \frac{r_2}{1-r_2};\ \beta = \frac{r_1}{1-r_1};\gamma = \frac{1-r_1r_2}{(1-r_1)(1-r_2)};\ \delta = \frac{1-r_2}{2-r_1-r_2}$$

$$X = 1 - \frac{[M_1]+[M_2]}{[M_{1,0}]+[M_{2,0}]};\ f_1 = \frac{[M_1]}{[M_1]+[M_2]}$$

Microstructure simulation

The resulting microstructure of a copolymer with an initial monomer ratio can be calculated by numerical integration according to Skeist[5] or with the Meyer Lowry equation. This gives values for total conversion X and the fraction of comonomer concentration f_1. To translate this to the composition in the copolymer F_1, the modified Mayo-Lewis equation can be used:

$$F_1 = \frac{r_1 f_1^2 + f_1 f_2}{r_1 f_1^2 + 2 f_1 f_2 + r_2 f_2^2}$$

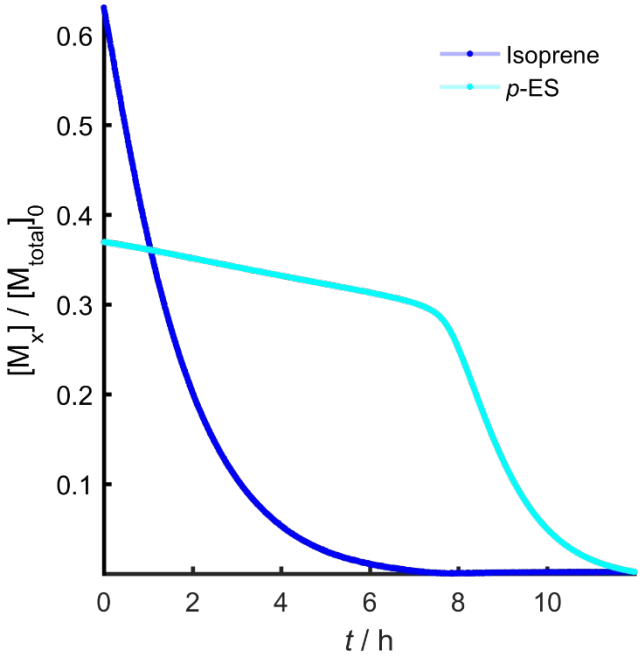

Figure S10. Monomer conversion as function of time for the copolymerization kinetics of isoprene and *p*-ES in C_6D_{12} at 23 °C, initiated with *sec*-butyllithium.

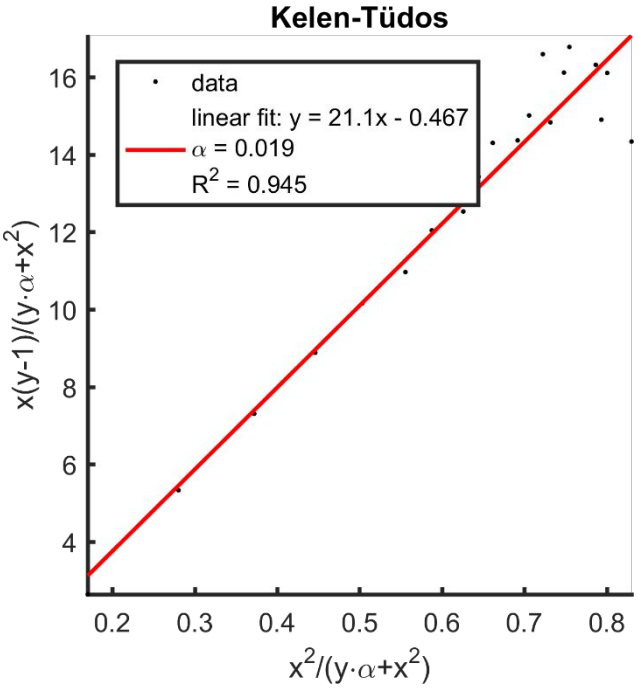

Figure S11. Kelen-Tüdos fit for the copolymerization kinetics of isoprene and *p*-ES in C_6D_{12} at 23 °C, initiated with *sec*-butyllithium.

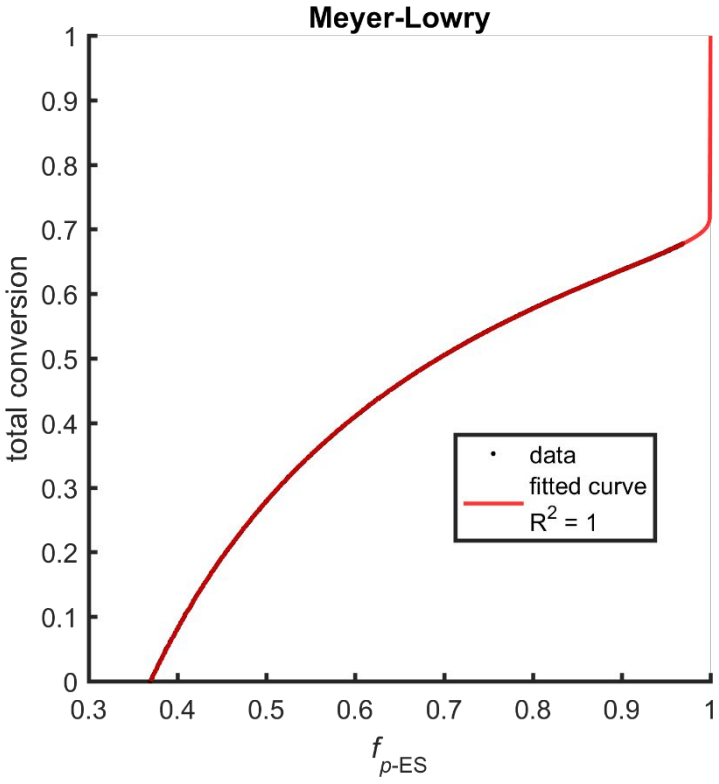

Figure S12. Meyer-Lowry fit for the copolymerization kinetics of isoprene and *p*-ES in C_6D_{12} at 23 °C, initiated with *sec*-butyllithium.

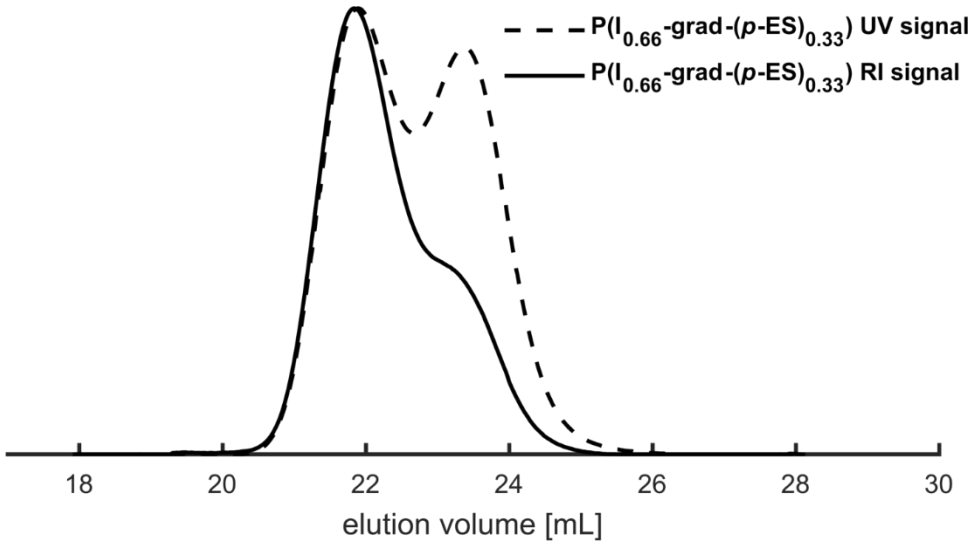

Figure S13. SEC traces UV signals (solid lines), RI signals (dashed lines), eluent: THF, PS standards of P(I-*grad*-(*p*-ES)) (66% I) from the copolymerization kinetics experiment. (M_n = 10,500 g mol^{-1}, $Đ$ = 1.23).

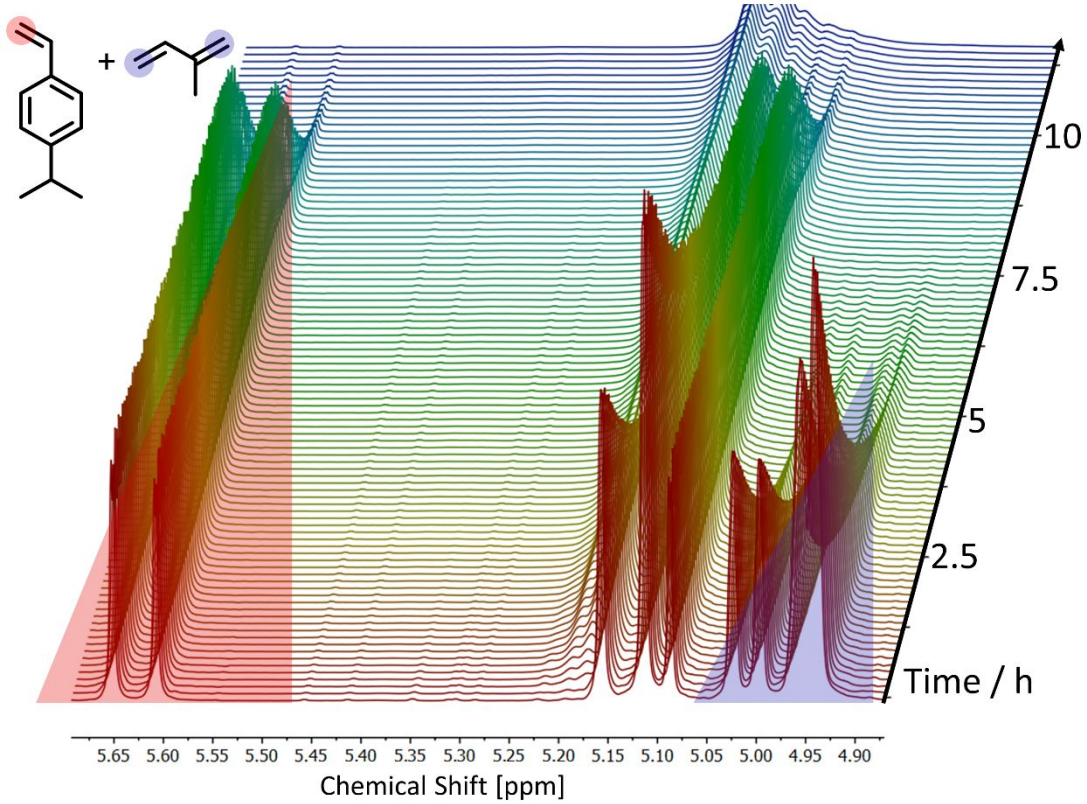

Figure S14. Stacked ^{1}H NMR spectra (400 MHz, C_6D_{12}) zoomed in region (5.7 – 4.85 ppm) as a function of time; *in situ* ^{1}H NMR kinetics characterization of the statistical copolymerization of isoprene and *p*-*i*PS.

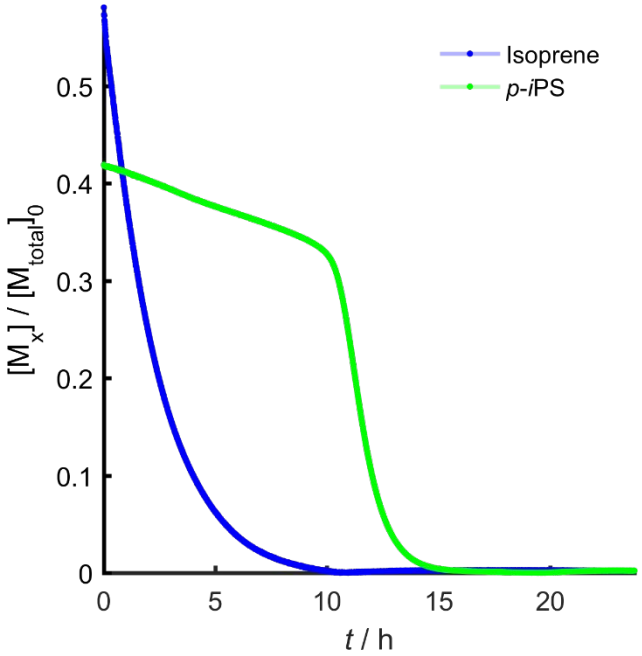

Figure S15. Monomer conversion as function of time for the copolymerization kinetics of isoprene and *p*-*i*PS in C_6D_{12} at 23 °C, initiated with *sec*-butyllithium.

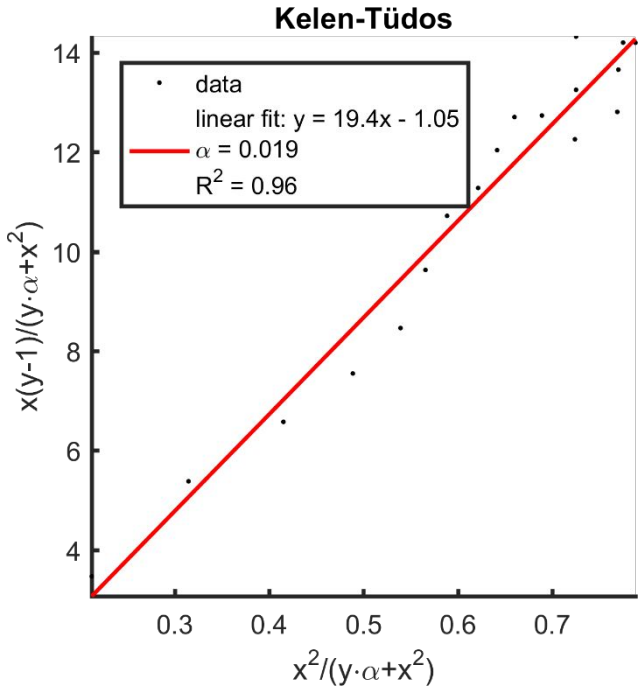

Figure S16. Kelen-Tüdos fit for the copolymerization kinetics of isoprene and *p*-*i*PS in C_6D_{12} at 23 °C, initiated with *sec*-butyllithium).

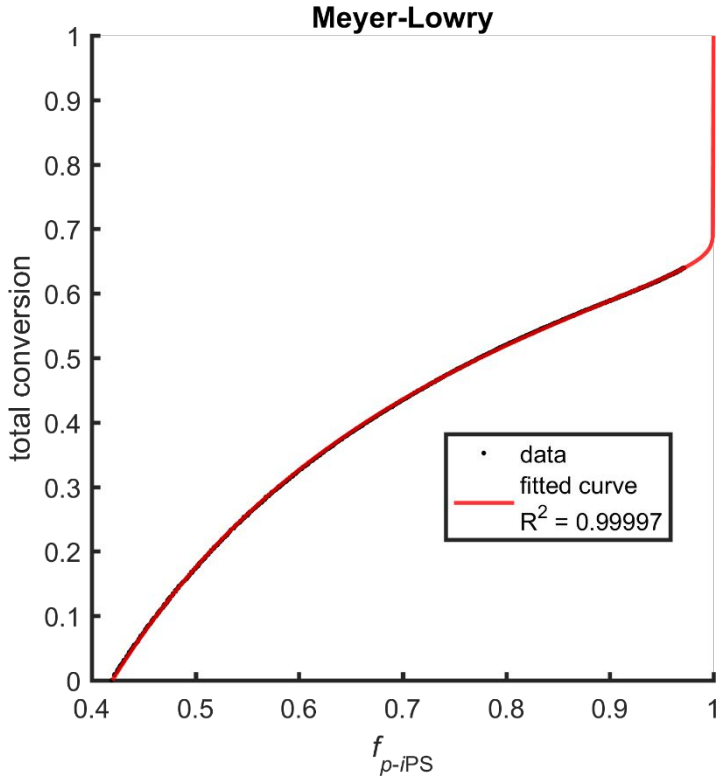

Figure S17. Meyer-Lowry fit for the copolymerization kinetics of isoprene and *p*-*i*PS in C_6D_{12} at 23 °C, initiated with *sec*-butyllithium).

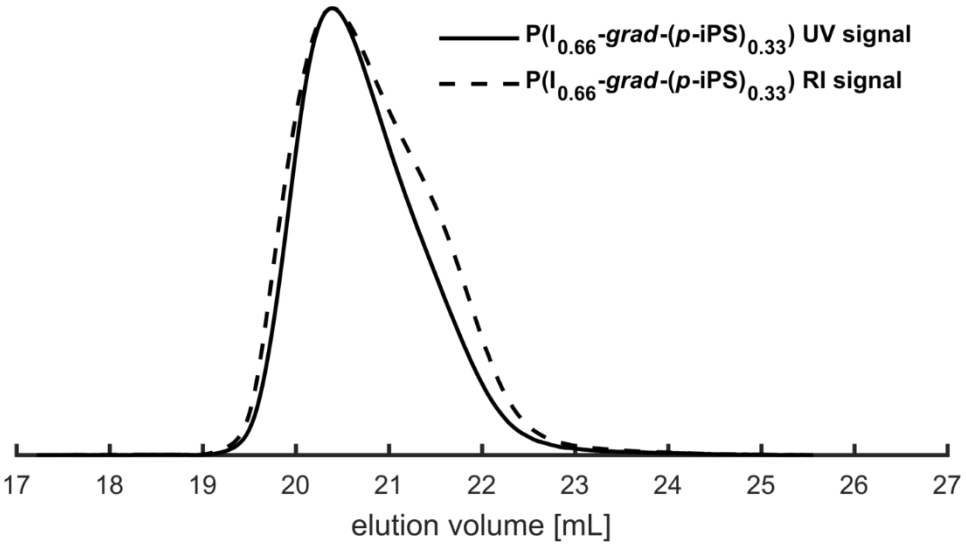

Figure S18. SEC traces UV signals (solid lines), RI signals (dashed lines), eluent: THF, PS standards of P(I-*grad*-(*p*-*i*PS)) from the copolymerization kinetics experiment (M_n = 29,300 g mol^{-1}, $Đ$ = 1.25).

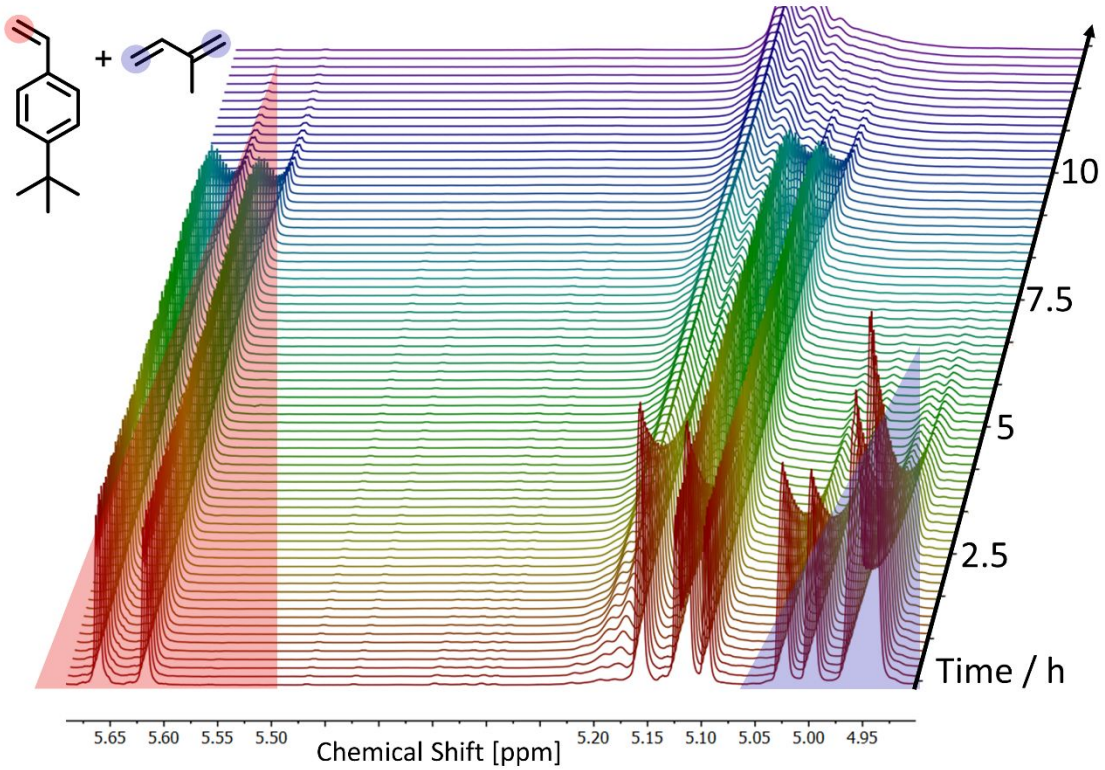

Figure S19. Stacked ^{1}H NMR spectra (400 MHz, C_6D_{12}) zoomed in region (5.7 – 4.85 ppm) as a function of time of the *in situ* ^{1}H NMR kinetics characterization of the statistical copolymerization of isoprene and *p*-*t*BS.

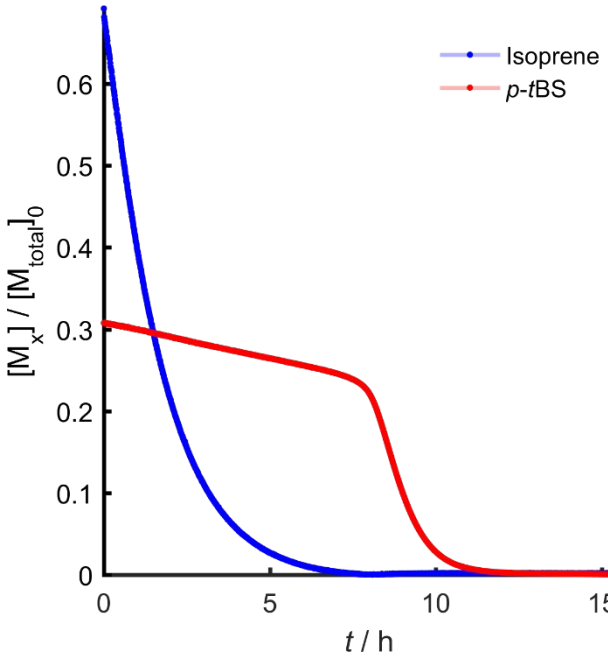

Figure S20. Monomer conversion as function of time for the copolymerization kinetics of isoprene and *p*-*t*BS in C_6D_{12} at 23 °C, initiated with *sec*-butyllithium.

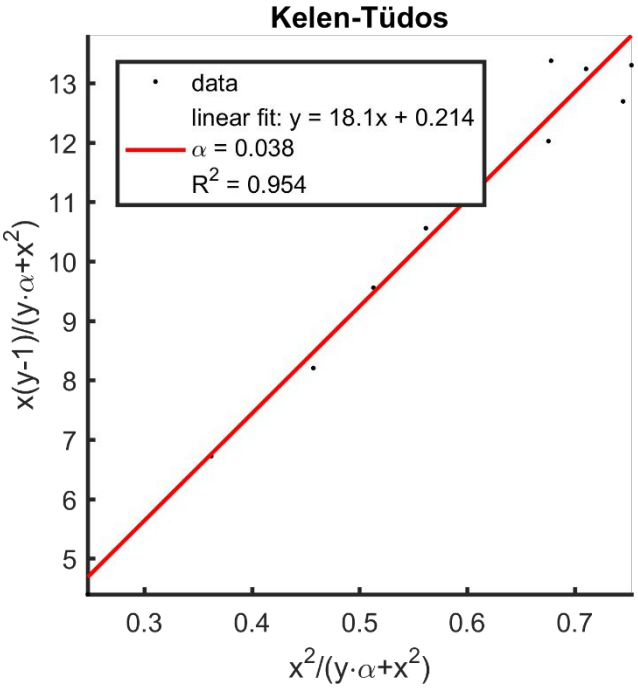

Figure S21. Kelen-Tüdos fit for the copolymerization kinetics of isoprene and *p*-*t*BS in C_6D_{12} at 23 °C, initiated with *sec*-butyllithium.

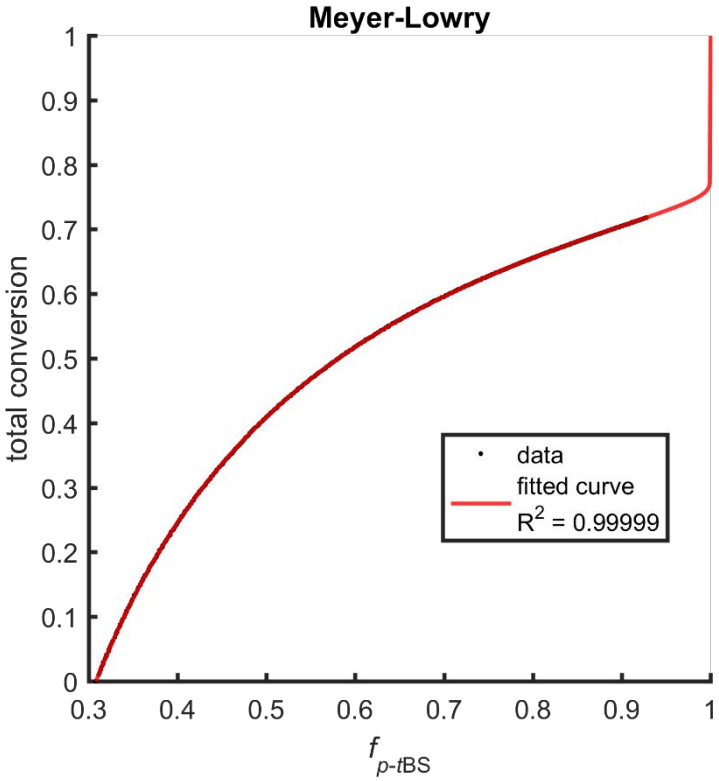

Figure S22. Meyer-Lowry fit for the copolymerization kinetics of isoprene and *p*-*t*BS in C_6D_{12} at 23 °C, initiated with *sec*-butyllithium.

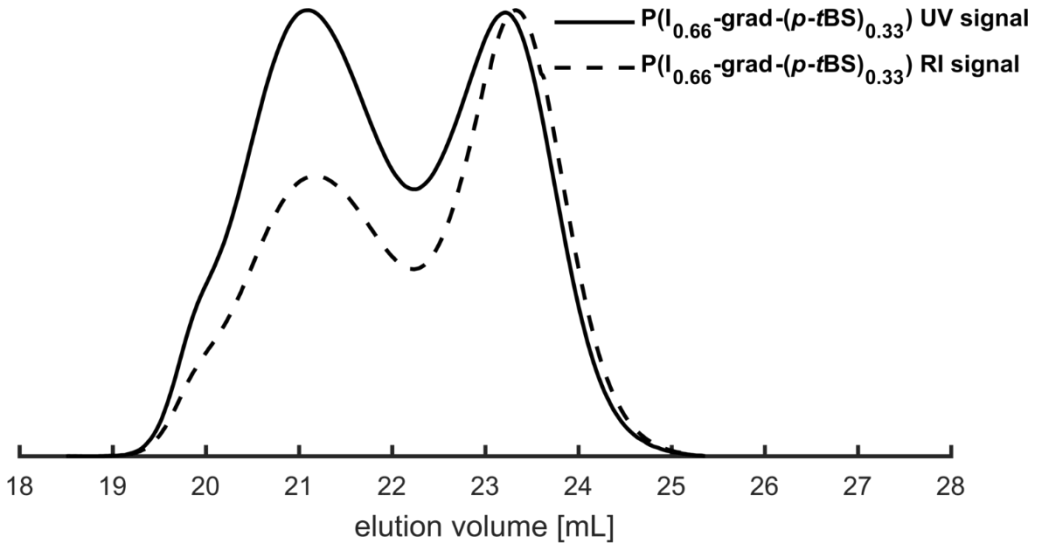

Figure S23. SEC traces UV signals (solid lines), RI signals (dashed lines), eluent: THF, PS standard; SEC trace of P(I-*grad*-(*p*-*t*BS)) from the copolymerization kinetics characterization (M_n = 11,600 g mol^{-1}, $Đ$ = 1.69).

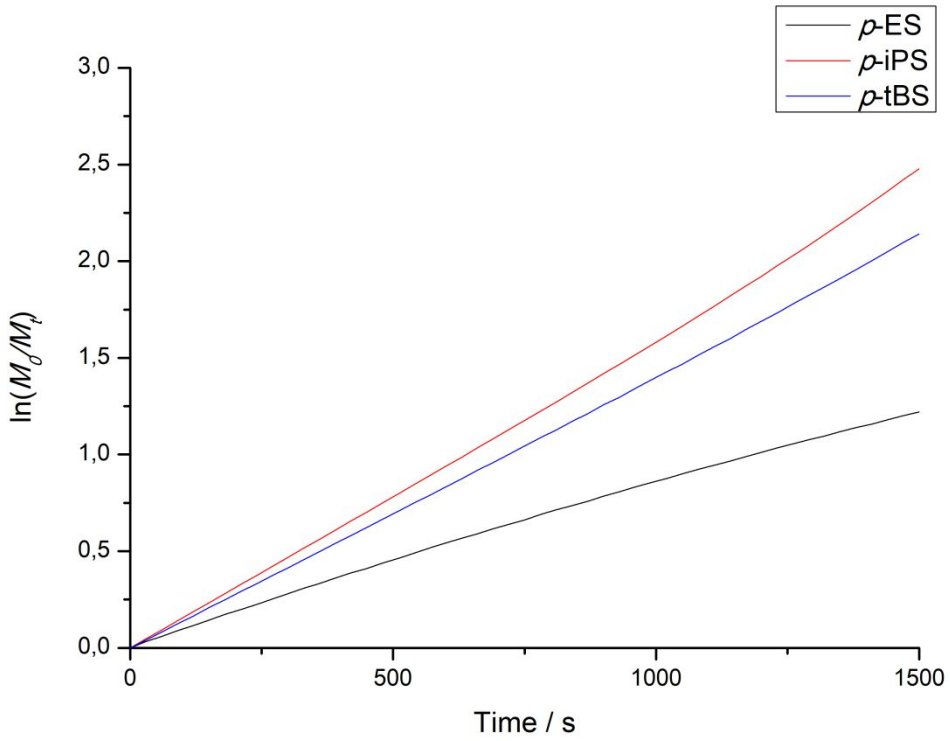

Figure S24. Pseudo-first-order time-conversion plots for the homopolymerization of *p*-ES, *p*-*i*PS and *p*-*t*BS in C_6D_{12} at 23 °C. (Due to the large amount of data points the plots appear like a solid line)

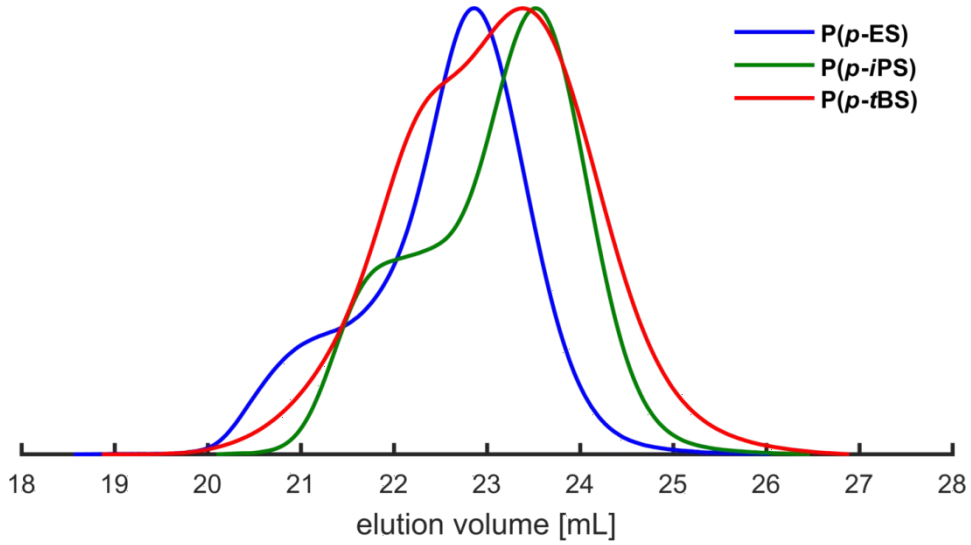

Figure S25. SEC traces (UV signals, eluent: THF, PS standards) of P(*p*-ES) (M_n = 9,180 g mol^{-1}, $Đ$ = 1.29), P(*p*-*i*PS) (M_n = 7,100 g mol^{-1}, $Đ$ = 1.22) and P(*p*-*t*BS) (M_n = 7,000 g mol^{-1}, $Đ$ = 1.30), samples from the homopolymerization kinetics characterization.

The traces in Figure S25 stem from the polymerization carried out in the NMR tubes during kinetics measurements. The bimodal character of the SEC traces obtained from the homopolymerization kinetics characterization was caused by traces of oxygen in the NMR tube.

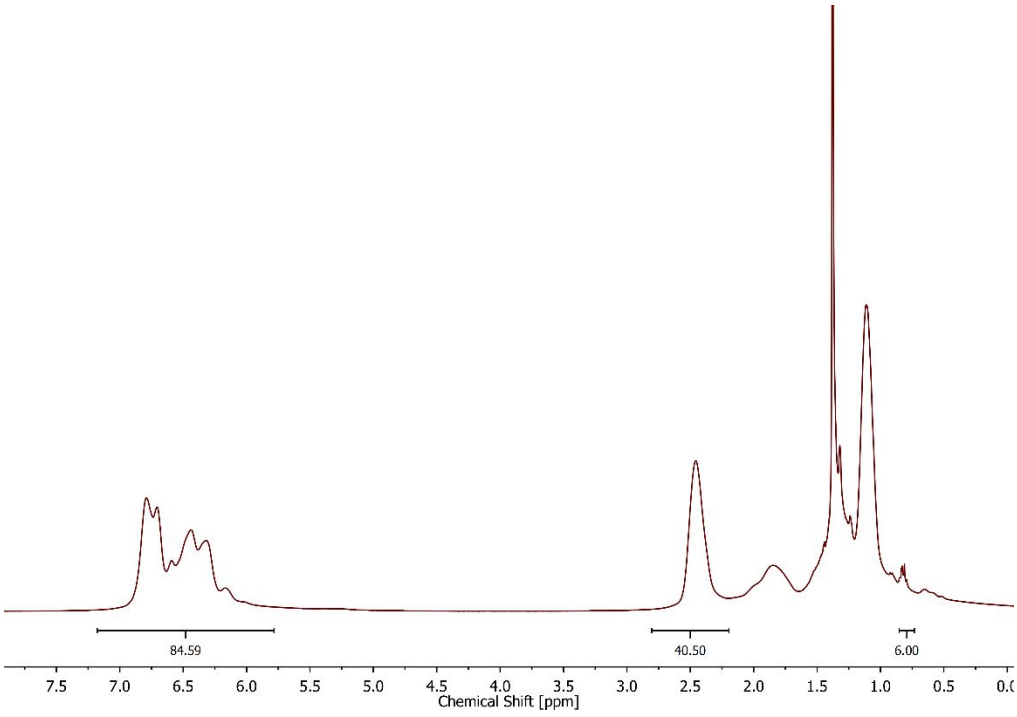

Figure S26. ^{1}H NMR spectrum of P(*p*-ES) (400 MHz, C_6D_{12}), of the homopolymerization kinetics sample.

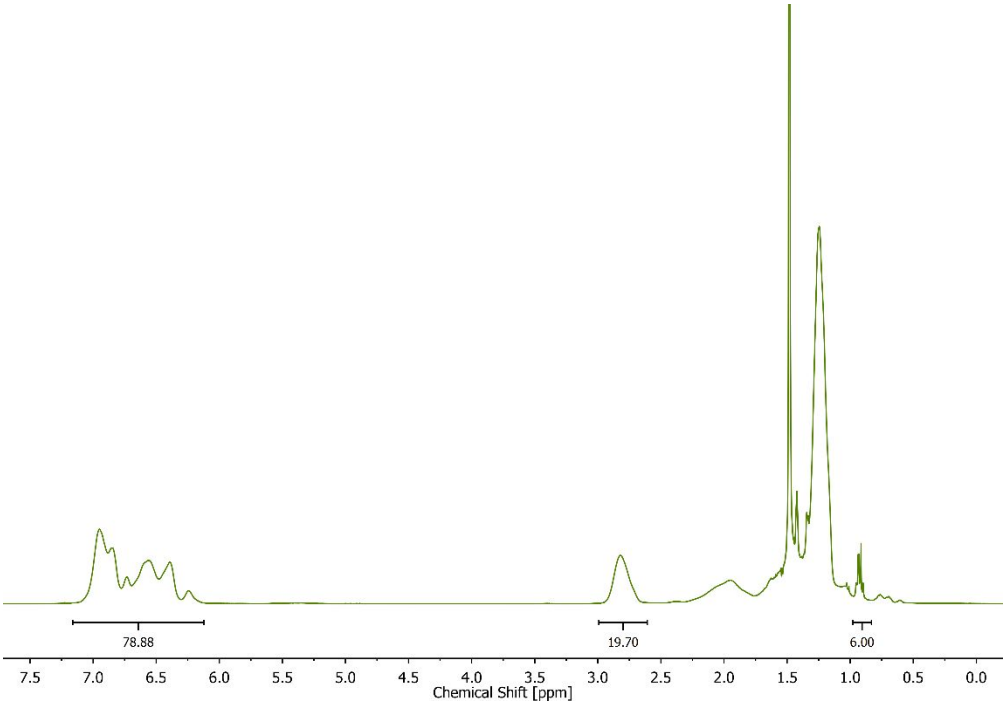

Figure S27. ^{1}H NMR spectrum of P(*p*-*i*PS) (400 MHz, C_6D_{12}) of the homopolymerization kinetics sample.

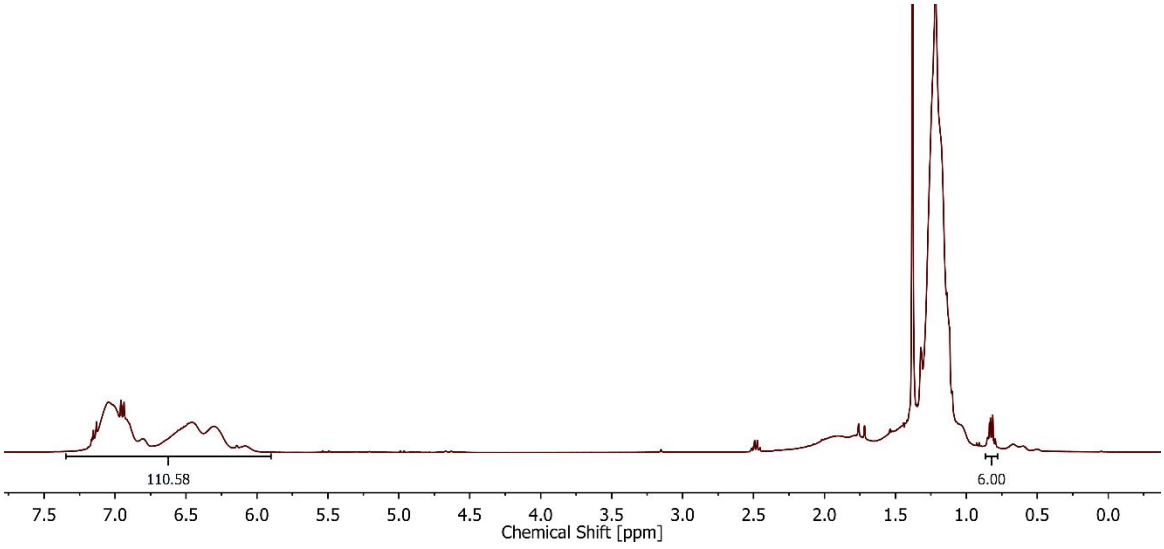

Figure S28. ^{1}H NMR spectrum of P(*p*-*t*BS) (400 MHz, C_6D_{12}) of the homopolymerization kinetics characterization, polymer formed in the NMR tube.

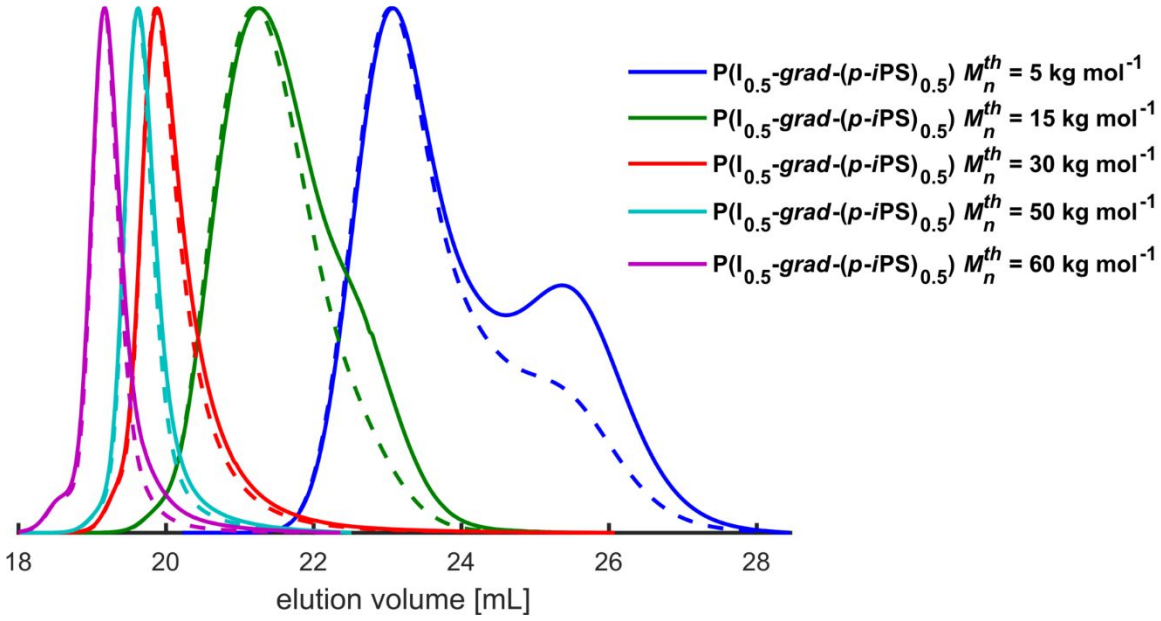

Figure S29: SEC traces, RI detector (solid lines), UV signals (dashed lines); eluent: THF, PS standards. High molecular weight (targeted 5,000 -60,000 g mol^{-1}) copolymers of isoprene and *p*-*i*PS.

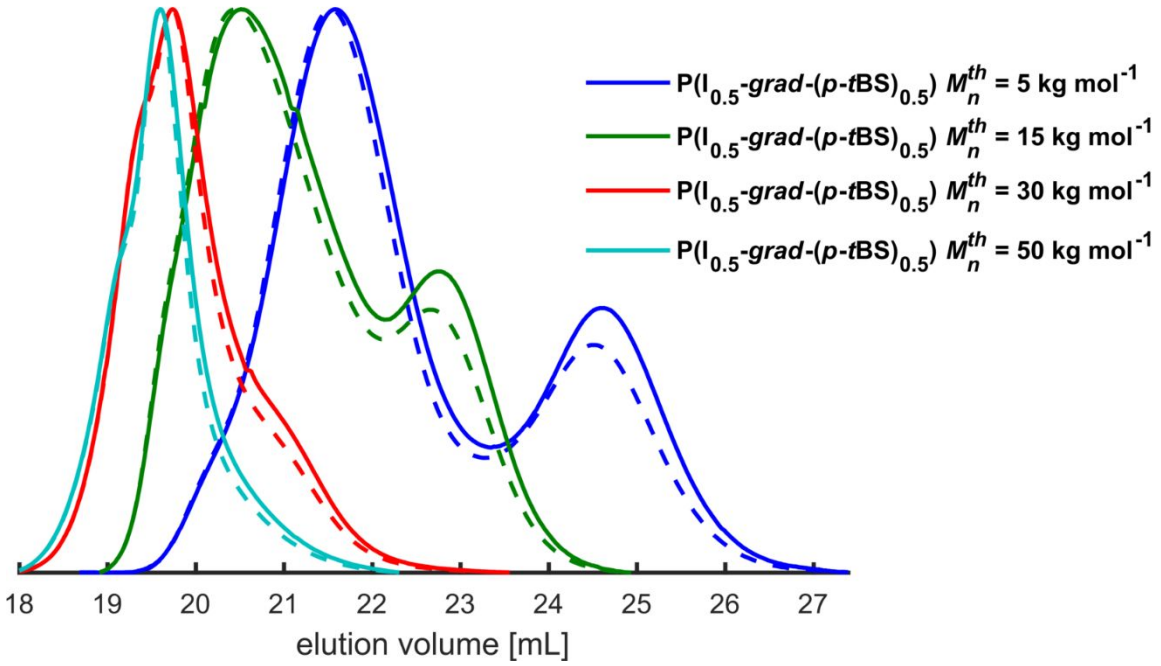

Figure S30. SEC traces RI detector (solid lines), UV detector (dashed lines), eluent: THF, PS standards. High molecular weight (targeted 5,000 -50,000 g mol^{-1}) copolymers of isoprene and *p*-*t*BS.

DFT Calculations

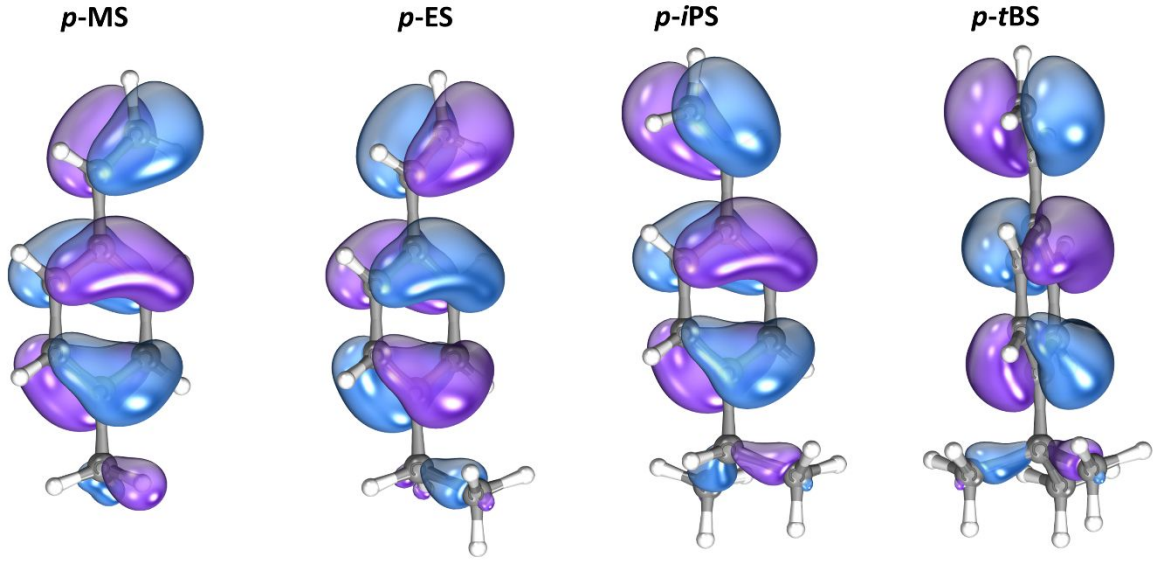

Figure S31. Calculated 3D geometries (HOMO orbitals) of *p*-MS, *p*-ES, *p*-*i*PS and *p*-*t*BS by DFT.

Table S2. *Para*-R bond length *p*-MS, *p*-ES, *p*-*i*PS and *p*-*t*BS as computed by DFT calculations.

Monomer	***p*-MS**	***p*-ES**	***p*-*i*PS**	***p*-*t*BS**
para-R bond length by DFT / pm	150.48	150.69	151.54	153.14

Ground state geometry of each styrene derivative was calculated using the B3LYP[6–9] density functional and the def2-TZVP [10,11] basis set. To take dispersion and long range interactions into account Grimme's D3 dispersion correction[12,13] and geometrical counterpoise correction[14] was applied.
The DFT calculations were performed on an Intel i5-7500 system with 16 GB RAM using the ORCA 3.0.2 software suite. [15]
To reduce the calculation effort the RIJCOSX[15] approximation method was used with the "GRIDX7" option. The SCF convergence was set to "VeryTight" while a grid setting of 6 was employed. For all ground states no imaginary frequency was detectable. The corresponding partial charges were calculated using the NBO method.[16,17]
Visualization of the orbitals were performed using IboView[18]
Typical ground state geometry optimization command input is shown below:

```
! B3LYP RIJCOSX D3BJ def2-TZVP def2-TZVP/J TIGHTOPT Opt Grid6
NOFINALGRID GridX7 freq NORMALPRINT GCP(DFT/TZ)
%pal nprocs 4 end
%maxcore 2000
%scf
SCFMode Direct
Convergence VeryTight
End
```

References

(1) PSS Polymer Standards Service GmbH. WinGPC UniChrom Benutzerdokumentation [Online], *01/2017*. www.pss-polymer.com.

(2) Mayo, F. R.; Lewis, F. M. Copolymerization. I. A Basis for Comparing the Behavior of Monomers in Copolymerization; The Copolymerization of Styrene and Methyl Methacrylate. *J. Am. Chem. Soc.* **1944**, *66* (9), 1594–1601.

(3) Blankenburg, J.; Wagner, M.; Frey, H. Well-Defined Multi-Amino-Functional and Stimuli-Responsive Poly(propylene oxide) by Crown Ether Assisted Anionic Ring-Opening Polymerization. *Macromolecules* **2017**, *50* (22), 8885–8893.

(4) Meyer, V. E.; Lowry, G. G. Integral and differential binary copolymerization equations. *J. Polym. Sci. A Gen. Pap.* **1965**, *3* (8), 2843–2851.

(5) Skeist, I. Copolymerization. *J. Am. Chem. Soc.* **1946**, *68* (9), 1781–1784.

(6) Becke, A. D. Density-functional thermochemistry. III. The role of exact exchange. *The Journal of chemical physics* **1993**, *98* (7), 5648–5652.

(7) Lee, C.; Yang, W.; Parr, R. G. Development of the Colle-Salvetti correlation-energy formula into a functional of the electron density. *Phys. Rev. B* **1988**, *37* (2), 785–789.

(8) Stephens, P. J.; Devlin, F. J.; Chabalowski, C. F.; Frisch, M. J. Ab Initio Calculation of Vibrational Absorption and Circular Dichroism Spectra Using Density Functional Force Fields. *J. Phys. Chem.* **1994**, *98* (45), 11623–11627.

(9) Vosko, S. H.; Wilk, L.; Nusair, M. Accurate spin-dependent electron liquid correlation energies for local spin density calculations: a critical analysis. *Can. J. Phys.* **1980**, *58* (8), 1200–1211.

(10) Weigend, F.; Ahlrichs, R. Balanced basis sets of split valence, triple zeta valence and quadruple zeta valence quality for H to Rn: Design and assessment of accuracy. *Physical chemistry chemical physics : PCCP* **2005**, *7* (18), 3297–3305.

(11) Schäfer, A.; Horn, H.; Ahlrichs, R. Fully optimized contracted Gaussian basis sets for atoms Li to Kr. *The Journal of chemical physics* **1992**, *97* (4), 2571–2577.

(12) Grimme, S.; Ehrlich, S.; Goerigk, L. Effect of the damping function in dispersion corrected density functional theory. *Journal of computational chemistry* **2011**, *32* (7), 1456–1465.

(13) Grimme, S.; Antony, J.; Ehrlich, S.; Krieg, H. A consistent and accurate ab initio parametrization of density functional dispersion correction (DFT-D) for the 94 elements H-Pu. *The Journal of chemical physics* **2010**, *132* (15), 154104.

(14) Kruse, H.; Grimme, S. A geometrical correction for the inter- and intra-molecular basis set superposition error in Hartree-Fock and density functional theory calculations for large systems. *The Journal of chemical physics* **2012**, *136* (15), 154101.

(15) Neese, F. The ORCA program system. *WIREs Comput Mol Sci* **2012**, *2* (1), 73–78.

(16) Reed, A. E.; Weinstock, R. B.; Weinhold, F. Natural population analysis. *The Journal of chemical physics* **1985**, *83* (2), 735–746.

(17) Nikolaienko, T. Y.; Bulavin, L. A.; Hovorun, D. M. JANPA: An open source cross-platform implementation of the Natural Population Analysis on the Java platform. *Computational and Theoretical Chemistry* **2014**, *1050*, 15–22.

(18) Knizia, G. Intrinsic Atomic Orbitals: An Unbiased Bridge between Quantum Theory and Chemical Concepts. *Journal of chemical theory and computation* **2013**, *9* (11), 4834–4843.